Chapter 11

Kinetic and Small Scale Solar Wind Physics

Thus far the origin, evolution, and large scale characteristics of the solar wind have been addressed using MHD theory and observations. In this lecture we consider aspects of the solar wind that either involve phenomena on small scales or that require the use of kinetic rather than fluid physics. Topics discussed include magnetic turbulence, acceleration at CIRs and transient interplanetary shocks, type III solar radio bursts, radial variations in the quantities predicted by the MHD theory of the solar wind, and pickup ions with origins in the interstellar medium and comets.

Aims and Expected Learning Outcomes

The **Aim** is to explore the roles of small scale structures and kinetic physics in the solar wind. This complements the evidence for MHD physics explaining well the solar wind's large scale structures and phenomena, as well as illustrating the connections between turbulence, shocks, particle acceleration, and plasma wave growth. These topics link Lectures 1-9 with the solar wind and lay some groundwork for Lecture 20.

Expected Learning Outcomes. You are expected to be able to

- Explain qualitatively what MHD turbulence is and describe its relevance to solar wind variability, shocks, particle acceleration, and heating of the solar wind.
- Discuss the physics of shock-drift acceleration and diffusive shock acceleration (Fermi acceleration) and interpret data in terms of these ideas.
- Describe conceptually the evolution of electron beams in the solar wind.
- Qualitatively compare the evolution of the solar wind magnetic field and the density, flow speed, and temperatures of the solar wind protons and electrons with MHD theory and give arguments as to why kinetic effects are important.
- Describe the physics of interstellar pickup ions in terms of particle motions, the mass-loading, slowing, and heating of the solar wind, and associated wave growth and turbulence.

11.1 MHD turbulence in the solar wind

The theory developed in Lecture 8 for the solar wind assumes a smooth, time invariant flow. In fact, the solar wind is a prime example of a medium with well developed, dynamically important turbulence . The term "turbulence" is used to describe small scale structures that cause the properties of the medium to vary in time and/or position with a large range of time scales. Turbulence is sometimes made up of multiple, broadband waves. Sometimes, however, the turbulence is not composed of waves, which are solutions of the (linear) dispersion equation, but are instead localized structures (e.g., eddies) or nonlinear entities.

Belcher and Davis [1971] first demonstrated that the solar wind contains MHD waves and turbulence: Figure 11.1 shows coupled variations in the three components of the magnetic field and fluid velocity of the solar wind. The correlation between

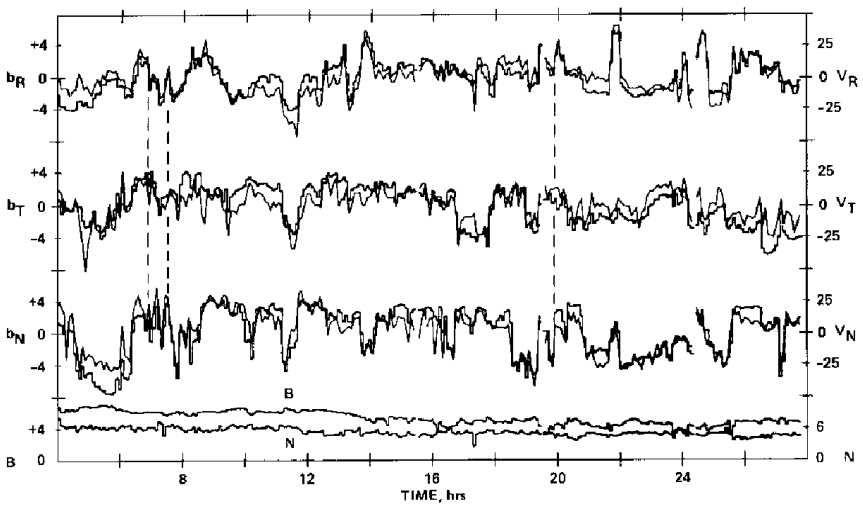

Figure 11.1: Alfven waves in the solar wind [Belcher and Davis, 1971]. The top three panels each show a different orthogonal component of the solar wind magnetic field and the associated (fluid) velocity component of the plasma. The bottom panel displays the magnitudes of the total magnetic field and flow speed.

the various components is very good and it should be noted that the total magnetic field strength and plasma density are essentially constant. Consistent with the theoretical properties derived in Lecture 2, these data are interpreted in terms of Alfven waves. (More recent investigations [e.g., Leamon et al., 1998] have also demonstrated the presence of components other than simple MHD wave modes in solar wind MHD turbulence.) In more detail, these waves primarily propagate outward from the Sun [Goldstein et al., 1995], suggesting a solar origin and possible connection with the heating of the corona.

MHD turbulence is usually investigated theoretically using the MHD equations. Statistical quantities are of primary use in understanding turbulence. Accordingly, correlation functions

$$R_{ij}(\tau) = \langle B_i(t) B_j(t+\tau) \rangle \ , \tag{11.1}$$

where τ is a time lag, and their associated power spectra play a central role in both theories and observations. The primary quantity considered is the power spectrum (or power spectral density), which is calculated by Fourier transforming R_{ij} to yield $R'_{ij}(\omega)$ and then forming $|R'_{ij}(\omega)|^2$.

Most turbulence theories involve the processes by which energy injected into a medium at large spatial scales is converted into motions at smaller and smaller spatial scales (or eddies) until reaching scales at which the turbulence energy interacts directly with individual plasma particles and causes heating (Figure 11.2). The

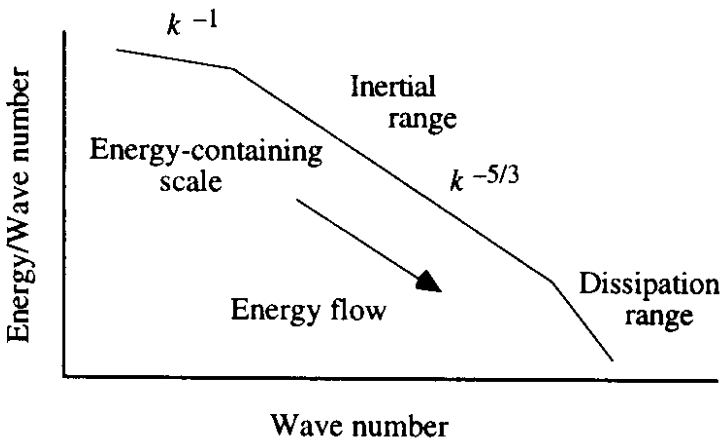

Figure 11.2: Schematic illustration of the power spectrum of MHD turbulence in the solar wind [Goldstein et al., 1995].

process by which wave energy moves to smaller wavenumbers is sometimes called a turbulent cascade. This process can be mimicked to some degree by stirring a fluid and watching it come into equilibrium. The range of wavenumbers over which the turbulence energy cascades to smaller wavenumbers is called the inertial range. Using both gasdynamic (GD) and MHD theory, it can be shown using energy balance arguments that the power spectrum in the inertial range should be a power law with spectral index in the range 3/2 – 5/3. Kinetic theory is required to understand the dissipation of the turbulence in the so-called "dissipation range" at small spatial scales. Leamon et al. [1998] first convincingly demonstrated the detection of the change in spectral index and wave properties expected in the dissipation range. Figure 11.3 shows both the inertial range and dissipation range of MHD turbulence in the solar wind for a characteristic period.

MHD turbulence is important for a number of reasons in space and solar physics. First, it accounts for many of the temporal and spatial variations in the fluid variables observed in the solar wind and other plasmas. Second, MHD turbulence is often vital in understanding the acceleration of particles at shocks, for instance in Fermi acceleration. Third, MHD turbulence can convert large scale fluid motions into heating of the thermal plasma. Fourth, generation of MHD turbulence can lead to the relaxation of unstable particle distributions, relevant to the discussions of comets and interstellar neutrals below. Finally, wave models for heating the solar corona often appeal to absorption of MHD turbulence. However, extrapolation of the power flux in solar wind MHD turbulence back to the corona does not remove existing difficulties in heating the corona [Goldstein et al., 1995].

11.2 Acceleration and transport of energetic particles

Lectures 1 and 5 introduced two acceleration processes relevant to particles in space plasmas: shock-drift acceleration involves particles undergoing plasma drifts parallel

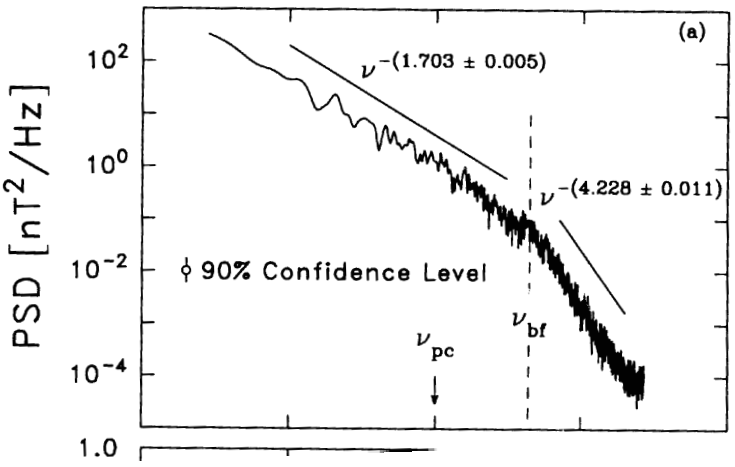

Figure 11.3: Typical spectrum of interplanetary magnetic field turbulence showing the inertial and dissipation ranges [Leamon et al., 1998].

or anti-parallel to the convection electric field, while diffusive shock acceleration (or Fermi acceleration) involves particles being scattered back and forth across a shock by magnetic turbulence. Evidence exists that each process is important at some interplanetary shocks and it is sometimes difficult to either rule out one process or to uniquely determine which process, if either, is relevant to a given set of observations.

Figure 11.4 [Burlaga et al., 1984; Smith, 1985] shows the flux of energetic ions (cosmic rays) observed during the passage of five evolved CIRs near 8 AU. Large changes in flux are frequently associated with the presence of the forward shock (S) or reverse shock (RS) of the CIRs (cf. the first two CIR shocks), providing strong evidence for particle acceleration at these shocks. However, there are also other changes in the particle flux, some of them abrupt and some of them gradual. Significant and abrupt drecreases in cosmic ray flux are observed during and after times of high magnetic field (and/or high levels of magnetic turbulence) between shock pairs. These minima are termed "Forbush" decreases and are associated with mirror reflection and magnetic drift of particles away from regions with high magnetic field. Here, indeed, large-scale quasi-global evolved CIRs with high magnetic field regions are believed to act as magnetic mirrors sweeping the cosmic rays outwards in front of them, leading to low cosmic ray counts after the high field regions. The slow rise in cosmic ray flux after these abrupt decreases is interpreted in terms of cosmic rays leaking in from the sides of the outward moving magnetic plugs.

Transient shocks driven by CMEs, and their ragions of enhanced magnetic field, can also produce large scale, global Forbush decreases in the cosmic ray flux, as discussed more in Lecture 20. There these structures are called Global Merged Interaction Regions or GMIRs.

Another aspect of Figure 11.4 is the evolution of the fast and slow streams and CIR structure by this distance (8 AU). Comparing Figure 11.4 with the cases in Lecture 10 (all of which were at smaller heliocentric distances), note that there is little structure in the plasma velocity at this distance: the flow speed is much more constant than at 1 AU and the CIR shocks are weak with only small velocity jumps from one side of the shock to the other. This is due to the CIR shocks reprocessing and homogenizing the plasma from near 1 AU outwards, slowing the fast streams and speeding up the slow streams, and converting the extra energy in

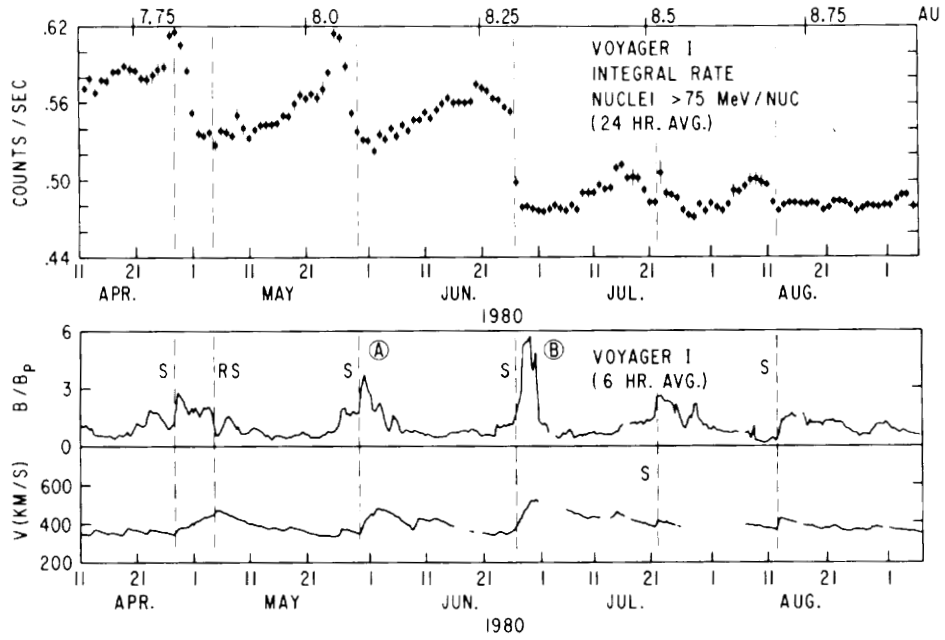

Figure 11.4: Voyager observations of cosmic rays at CIRs near 8 AU [Burlaga et al., 1984; Smith, 1985]. The middle panel shows the ratio of the observed magnetic field strength to that predicted for the Parker spiral model. The first two shocks are associated with increases in the cosmic ray flux but followed by Forbush decreases in the high field regions behind the shocks.

fast streams into plasma heating, magnetic turbulence, particle acceleration, and a more uniform outflow. In contrast, magnetic structures have been enhanced. These persist into the outer heliosphere. As discussed more in Section 11.4, CIRs are currently believed very important in determining how the plasma temperature and magnetic turbulence vary with heliocentric distance once beyond a few AU, as are interstellar pick-up ions (Section 11.5).

Shock-drift acceleration (Lecture 5.4) is predicted to be most effective for quasi-perpendicular shocks (where the angle θ_{Bn} between the shock normal and field $\mathbf{B}$ is close to 90 degrees) with the energy gain being sensitively dependent on θ_{Bn} but restricted to factors ≤ 10. See equation (5.27):

$$v_{\parallel}^{f} = 2V_{sh} \sec\theta_{Bn} - v_{\parallel}^{i} \ . \tag{11.2}$$

The requirement that θ_{Bn} be > 80 degrees for significant acceleration means that the accelerated particles will tend to be concentrated relatively close to the shock. This is because the field lines are almost perpendicular to the shock surface so that the particles find it difficult to propagate too far upstream from the shock (into the "foreshock" region). Figure 11.5 illustrates this tendency.

Diffusive shock acceleration (Lecture 5.5) can be important for both quasi-parallel and quasi-perpendicular shocks. In the quasi-parallel case the accelerated particles and the waves they produce can escape to large distances from the shock, thereby filling a large foreshock volume. Diffusive shock acceleration tends to produce a power-law distribution with

$$f(p) = Ap^{-b} = CE^{-b/2} \tag{11.3}$$

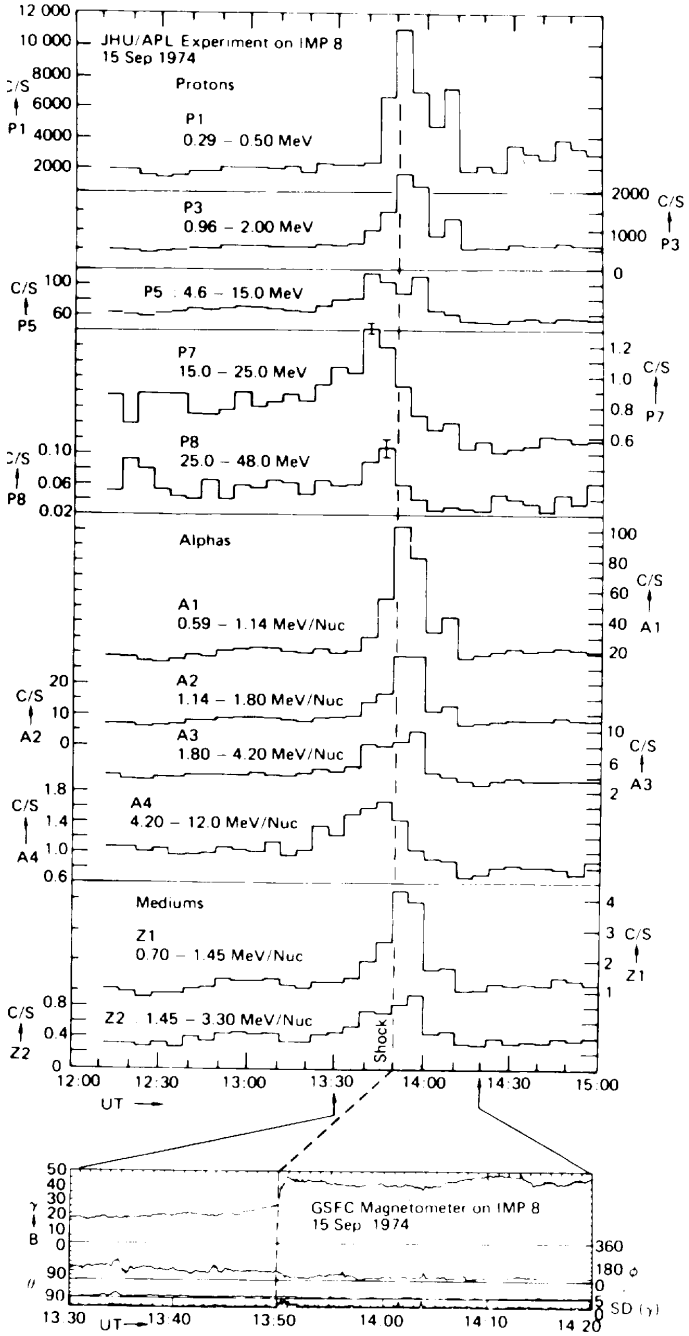

Figure 11.5: Count rates for protons, alpha particles and "medium mass" nuclei near an almost perpendicular ($\theta_{Bn} \sim 88$ degrees) transient interplanetary shock [Armstrong et al., 1985]. The peaking of the count rates near the shock is qualitatively consistent with shock drift acceleration.

where

$$b = 3r/(r-1) \tag{11.4}$$

and

$$r = \frac{n_{down}}{n_{up}} \tag{11.5}$$

is the density jump across the shock. For a strong shock ($r = 4$), then $f(p) \propto p^{-4} \propto E^{-2}$; weaker shocks produce steeper spectra. Figure 11.6 illustrates the predicted power-law dependence of the distribution function downstream of a travelling interplanetary shock [Gosling et al., 1981].

Diffusive acceleration also predicts an exponential increase in the particle flux with decreasing distance to the shock. Figure 11.7 illustrates this behaviour [Scholer et al., 1983]. MHD waves driven by the accelerated particles have also been detected but are not discussed here. However, a detailed and very successful application of diffusive shock acceleration to an interplanetary shock (addressing both the waves and particles) is described by Kennel et al. [1986] and should be consulted by interested readers.

11.3 Type III solar Radio bursts

Type III solar radio bursts are an example of kinetic physics in the solar wind that involve intrinsic temporal variations and a coupling of small spatial scales to large spatial scales. They are associated with streams of energetic electrons ($v/c \sim 0.1 - 0.5$) released onto open field lines during solar flares which naturally develop a beam distribution by time-of-flight effects and then drive Langmuir waves and radiation near multiples of the plasma frequency. Type III bursts illuminate many interesting and important questions regarding the evolution of electron beams and Langmuir waves in plasmas. They also can be used to trace the Parker spirals characteristic of interplanetary magnetic field lines. They were discussed in some detail in Lecture 4.

11.4 Arguments for kinetic physics in radial variations of solar wind parameters

Many global aspects of the solar wind flow are well described by the fluid theory developed and used in Lectures 3 – 7 and 10. However, even some of these global aspects point to a need to directly consider the kinetic and not fluid nature of the plasma. These points are now illustrated in some detail.

Figure 11.8 [Belcher et al., 1993] shows that the solar wind plasma density follows the simple $n_{sw} \propto R^{-2}$ fall-off predicted by fluid theory, and on more general grounds by global mass conservation. Similarly, Parker's theory for the solar wind predicts that v_{sw} asymptotes to a constant value within about 10 solar radii and then remains constant further from the Sun. Richardson et al. [1995] show that this result is consistent with Voyager data (except perhaps beyond 20 AU where mass loading by interstellar pickup ions may cause a small slowdown - see below). Similarly the magnetic field is well described by Parker's MHD theory, as shown in Figure 11.9 [Burlaga et al., 1998] taking into account solar cycle variations in the solar wind speed at the spacecraft location. Thus, the magnetic field and the zeroth and first moments of the particle distribution function follow the predictions of MHD theory very well.

The situation is different for the second moments (e.g., temperatures) of the solar wind electrons and ions, although the different results of competing scientific teams suggest that no consensus has been reached on these issues. The first and most

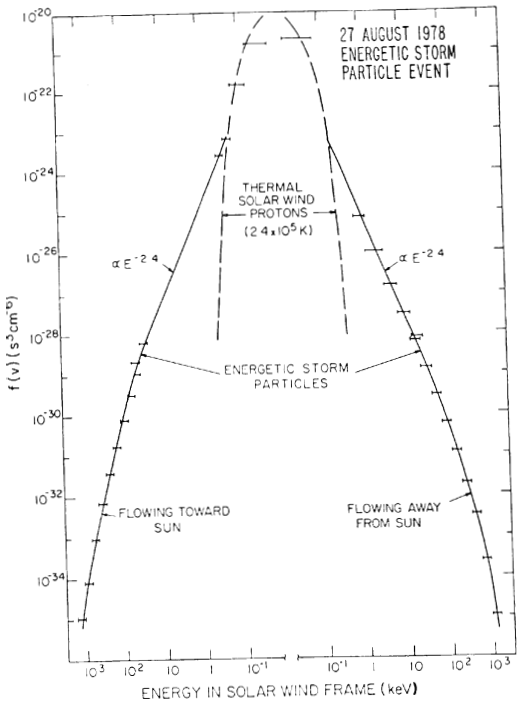

Figure 11.6: Measured distribution function of interplanetary protons in the solar wind frame behind a transient interplanetary shock [Gosling et al., 1981; Scholer, 1985]. The distribution is composed of a thermal core of solar wind protons plus superposed power law tails consistent with diffusive shock acceleration.

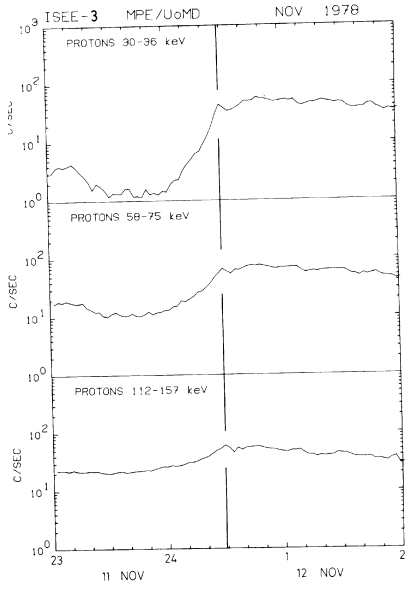

Figure 11.7: Exponential increases in the count rate of energetic particles with decreasing distance to an interplanetary shock, qualitatively consistent with diffusive shock acceleration [Scholer et al., 1983].

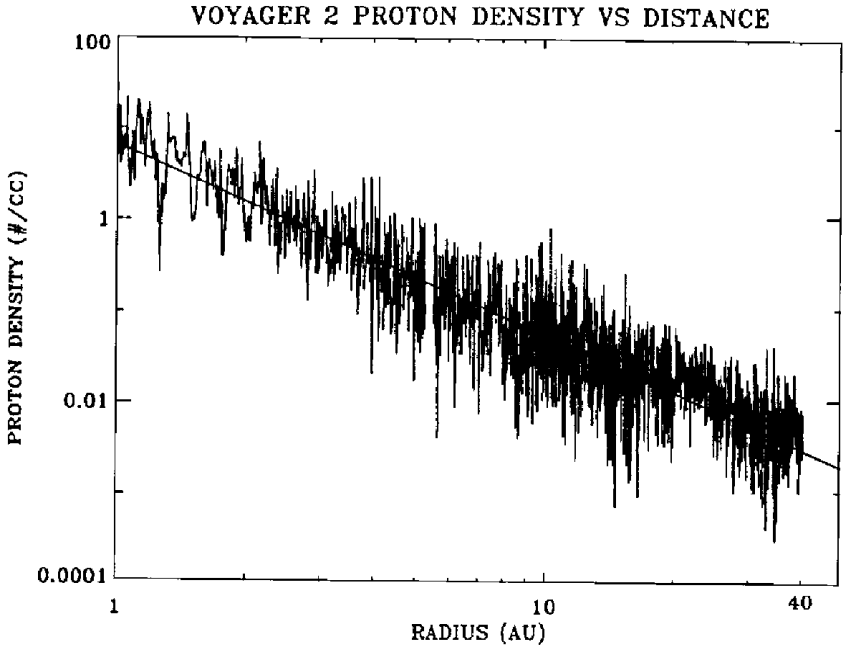

Figure 11.8: The solar wind plasma density as a function of heliocentric distance R [Belcher et al., 1993].

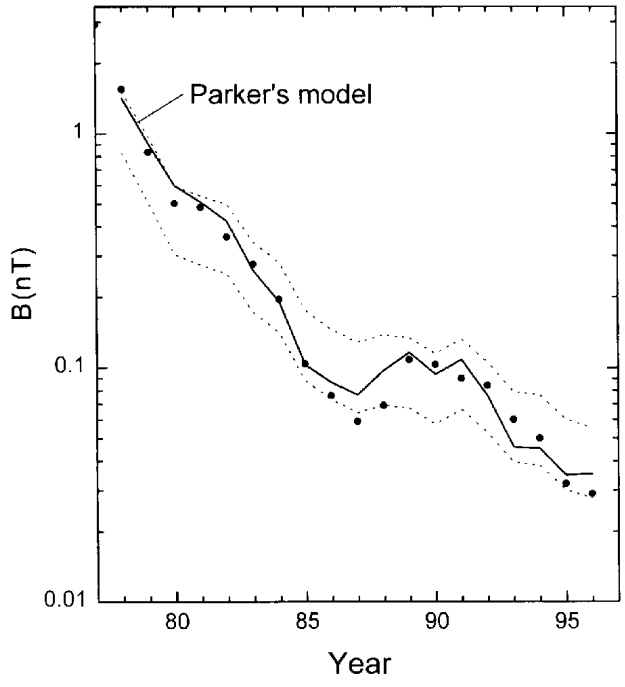

Figure 11.9: Voyager 1 observations of the magnetic field strength versus time (solid dots) and Parker's prediction (solid curve) taking into account variable solar wind speed and variable source fields in the photosphere [Burlaga et al., 1998]. The dotted curves show Parker's predictions for variable source fields but constant solar wind speeds of 800 and 400 km s^{-1} for the bottom and top curves, respectively.

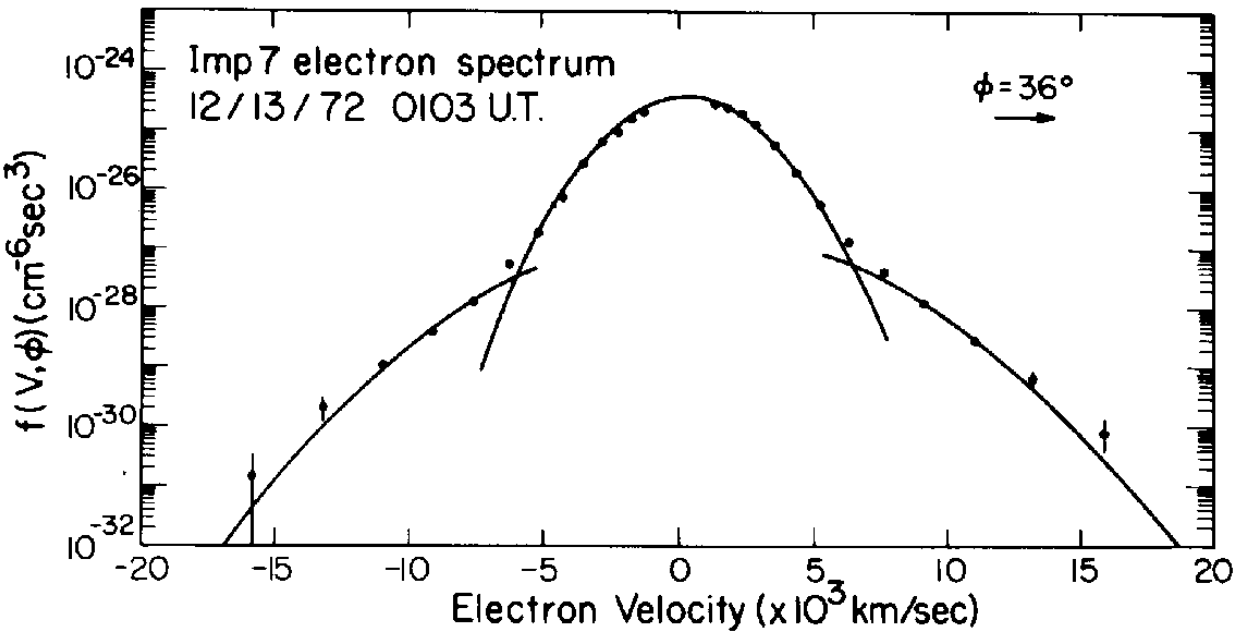

Figure 11.10: A cut through a solar wind electron distribution along the magnetic field direction [Feldman, 1979]. The two solid curves are two bi-Maxwellian functions which best fit the core and halo electrons at low and intermediate energies, respectively.

obvious illustration of this difference is that the ratio of electron to ion temperature in the solar wind near 1 AU is typically $T_e/T_i \sim 3$. If these species were strongly thermally coupled then they would have identical temperatures.

A second illustration is provided by the different variations of the ion and electron temperatures with heliocentric distance. While electrons tend to be hotter than the ions near 1 AU, in Lecture 7 it was shown that protons (and other ions) tend to be much hotter than electrons in the solar corona: protons must cool much faster than electrons with increasing heliocentric distance. To see this more quantitatively, assume that the temperatures vary in a power-law fashion with R, with $T = T_0(R/R_0)^{-\gamma}$, and then calculate the power law indices γ for each species. Using $T_e = T_i = 10^6$ K at 10 solar radii and $T_e = 1.5 \times 10^5$ K and $T_i = 5 \times 10^4$ K at 1 AU (215 solar radii) yields $\gamma_i = 1.0$ and $\gamma_e = 0.6$. Moreover, analyses of observational data suggest that these indices are $\gamma_i \sim 0.6 \pm 0.1$ between 1 and 10 AU and $\gamma_e \sim 0.2 - 1.2$ for the same range of heliocentric distances.

Third, comparing these empirical estimates for γ_i and γ_e with theory is instructive. The fluid theories in Chapter 8 yield $\gamma = 4/3$ for adiabatic flow and $\gamma = 0$ for isothermal flow. How can these differences be explained in the context of MHD or two-fluid theory?

The non-fluid nature of the electron distribution is illustrated in Figure 11.10, where it can be seen that the distribution is well-represented as the sum of two approximately Maxwellian components: a relatively dense and cold "core" component and a relatively hot and dilute "halo" component. The core and halo electrons drift relative to one another, resulting in a net heat flux outward away from the Sun. The detailed variations of the solar wind heat flux and the core and halo distributions are not yet understood. The way forward, however, is widely believed to require

the use of kinetic physics and wave-particle interactions.

11.5 Interstellar pickup ions

Not all solar wind protons reach the interstellar medium (ISM) as protons. Instead, a small fraction undergo a collisional charge-exchange interaction with neutral hydrogen atoms from the ISM, and so reach the I SM as neutral H atoms. This interaction corresponds to an electron jumping from one proton to another and can be written as

$$p^+(\mathbf{v}_{sw}) + H(\mathbf{v}_{ISM}) \rightarrow H(\mathbf{v}_{sw}) + p^+(\mathbf{v}_{ISM}) \ . \tag{11.6}$$

Here $\mathbf{v}_{sw}$ represents the solar wind velocity and $\mathbf{v}_{ISM}$ represents the velocity of the interstellar medium relative to our solar system, which has a magnitude of only 25 km s^{-1}. From the viewpoint of the solar wind (Figure 11.11), then, a proton near zero velocity is suddenly replaced by a (interstellar) proton which is "born" with an initial velocity approximately equal to $-\mathbf{v}_{sw}$. This new proton, however, must also start to gyrate around the magnetic field. In the case of solar wind flow perpendicular to $\mathbf{B}_{sw}$ this means that the initial gyrospeed is v_{sw} and so the "picked-up" proton moves on a circle of radius v_{sw} centered on the solar wind ions. In the Sun's frame then the energy of the pick-up ion varies between zero and 4 times the solar wind proton energy. In general, the maximum energy is

$$E_{max} = 4E_{sw}^2 \sin^2\theta = 2m_\alpha v_{sw}^2 \sin^2\theta \ , \tag{11.7}$$

where θ is the angle between the magnetic field direction and $\mathbf{v}_{sw}$. It may be asked where this extra energy has come from? The answer is "from the convection electric field when it accelerates the pickup ion into its gyromotion". The consequence is, of course, that the solar wind flow must slow down to accommodate this energy flow into pick-up ions. Furthermore, the interstellar pick-up ions will appear as a heated component with "thermal" energy well above the thermal energy of the solar wind ions, thereby appearing to increase the temperature of the solar wind ions. Both this mass-loading and the heating should change the evolution of the solar wind at large heliocentric distances (see below). Finally, the ring distribution of pickup ions has sizeable gradients $\partial f/\partial v_\parallel$ and $\partial f/\partial v_\perp$ and is theoretically unstable to the growth of MHD and other waves (see Lecture 4), with specific ranges of frequencies and wavevectors.

In the last 15 years detection of interstellar pickup ions has become routine using advanced detectors on the Ulysses and ACE spacecraft. Figure 11.12 shows the energy distribution of interstellar pickup protons and He^+ ions [Gloeckler et al. 1993]. Theoretically pickup protons are expected to be important for the evolution of the solar wind beyond about 5 AU. Experimental evidence for pickup ions (and CIRs) quantitatively affecting the solar wind is provided in Figures 11.13 [Matthaeus et al., 1999] and 11.14 [Richardson et al., 1995], which show the apparent heating and slowing of the solar wind. In both cases the effects of pickup ions are semi-quantitatively consistent with the observations.

11.6 Pickup ions at comets

Comets provide another opportunity to discuss MHD turbulence and pickup ions. In this case the pickup ions are produced by photoionization or charge-exchange of water molecules evaporated from the comet's surface. Once again, the cometary particles are moving very slowly relative to the solar wind but are picked up by the solar wind with large gyrospeed and a varying energy with maximum value given by (11.7). The ring-beam distribution of pickup water ions then excites large

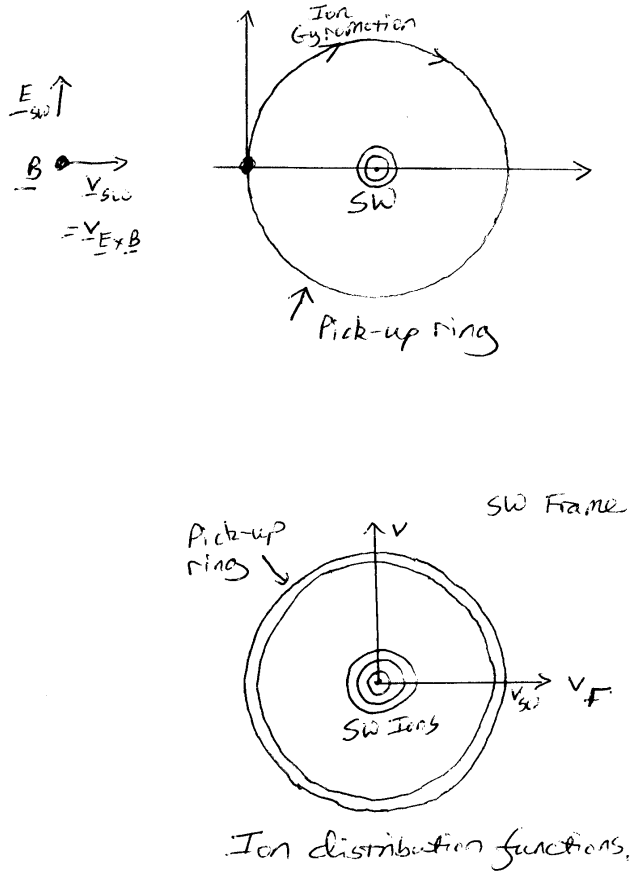

Figure 11.11: The top portion shows the pickup ring, solar wind flow, and the directions of the solar wind velocity, electric, and magnetic fields in the **solar** frame: pickup ions are born at (essentially) zero velocity but are then sped up by the convetion electric field to develop a gyrospeed equal to v_{sw}. The bottom portion is a contour plot of the ion velocity distribution in the solar wind frame, showing the solar wind protons near zero velocity and the pickup ions in a ring distribution.

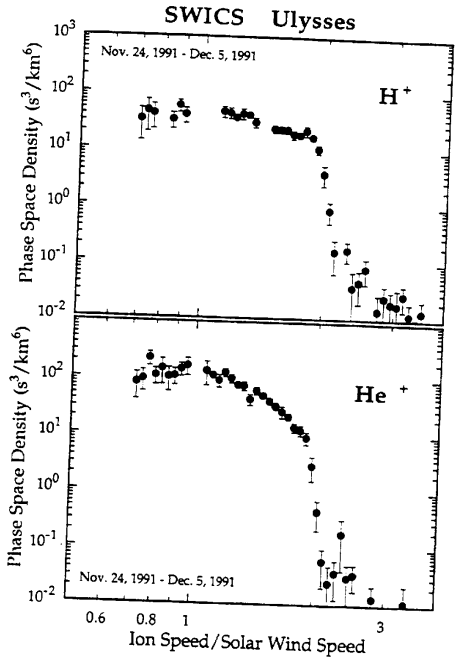

Figure 11.12: The phase space density of interstellar pickup protons as a function of v/v_{sw} observed in the spacecraft frame by Ulysses at 4.2 AU [Gloeckler et al., 1993].

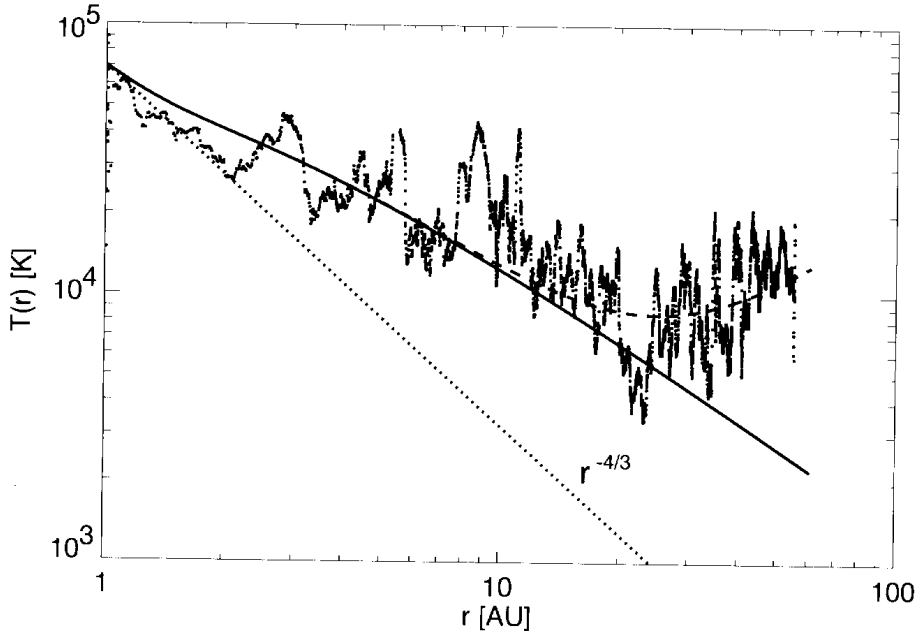

Figure 11.13: Proton temperature data observed by the Voyager 2 spacecraft (jagged curve) are compared with the predictions of adiabatic cooling (dotted line) and a turbulent heating model including heating by CIRs alone (solid curve) and by pickup ions and CIR heating (dashed curve) [Matthaeus et al., 1999].

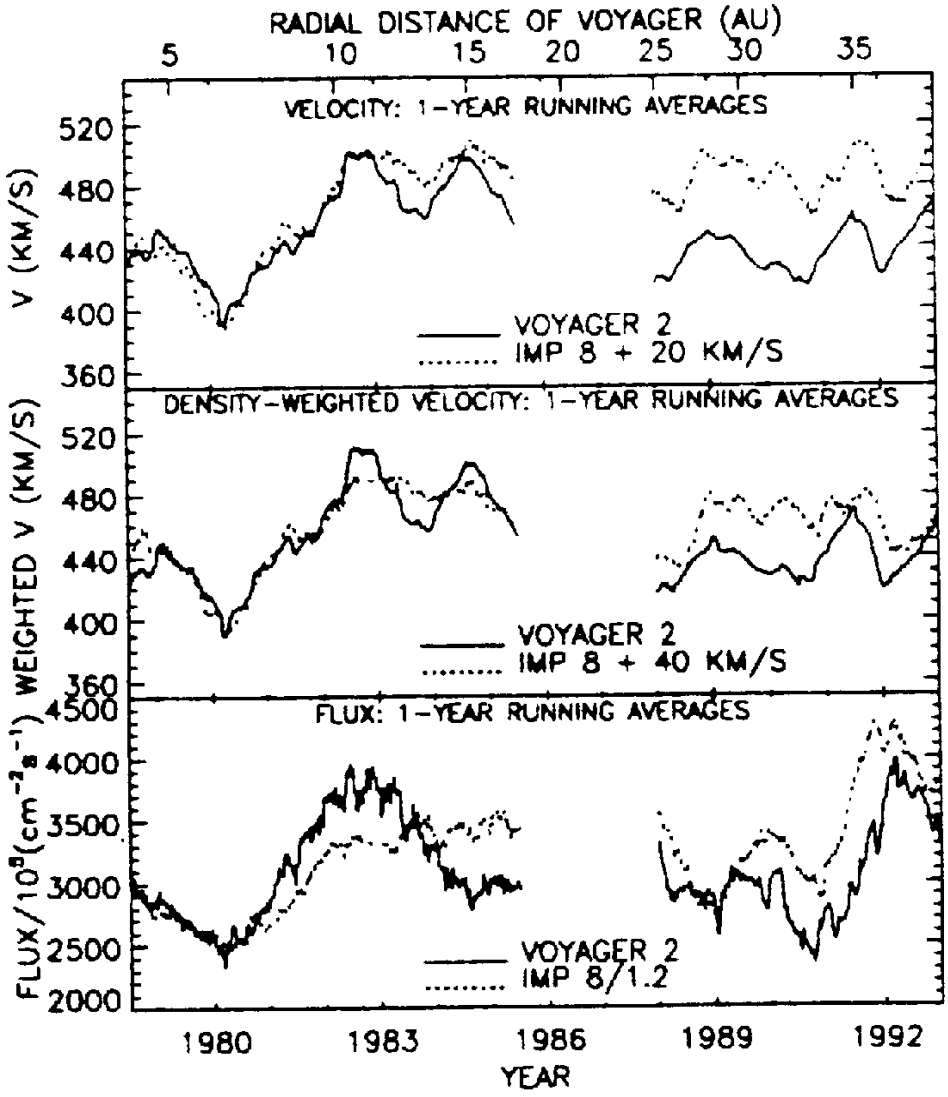

Figure 11.14: The speed, density-weighted speed, and number flux for solar wind protons measured by the Voyager 2 spacecraft in the outer solar system (solid curve) and by the IMP 8 spacecraft at 1 AU (dotted curve) [Richardson et al., 1995]. Note that the solar wind speed is approximately constant with heliocentric distance but with the suggestion of a small decrease beyond about 15 AU.

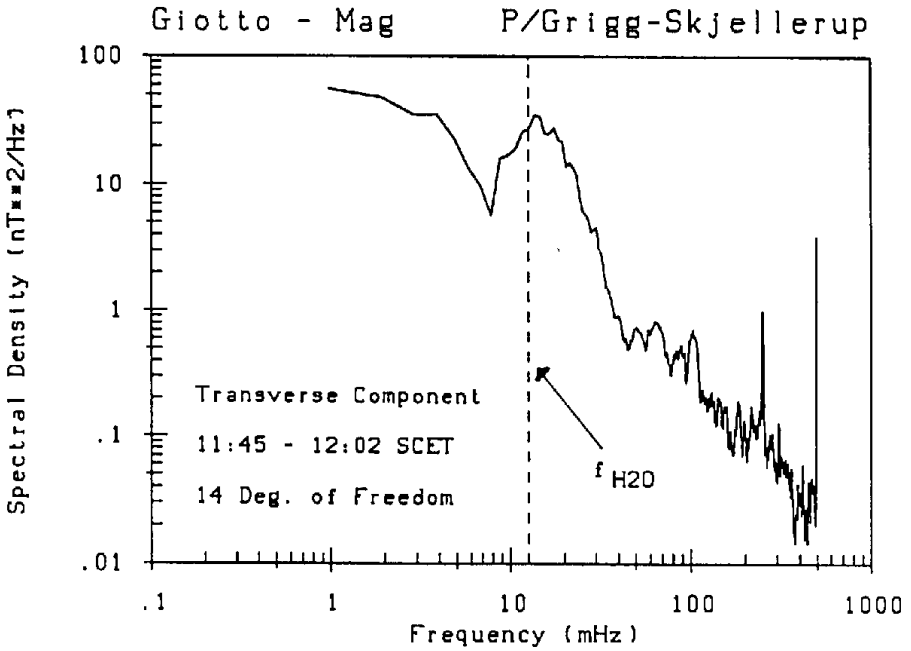

Figure 11.15: Sample magnetic power spectrum measured by GIOTTO sunward of Comet Grigg-Skjellerup [Glassmeier and Neubauer, 1993]. The dashed line shows the cyclotron frequency for water ions.

amplitude MHD waves, as well as other higher frequency waves such as ion acoustic waves. Figure 11.15 [Glassmeier & Neubauer, 1993] show the input of power near the water ion cyclotron frequency and a turbulence cascade to smaller wavelengths.

11.7 References

- Armstrong, T.P., M.E. Pesses, and R.B. Decker, Shock drift acceleration, in *Collisionless Shocks in the Heliosphere: Reviews of Current Research*, Eds. B.T. Tsurutani and R. G. Stone, AGU, 271, 1985.
- Belcher, J.W., and L. Davis, Jr., Large amplitude Alfven waves in the interplanetary medium, **J. Geophys. Res.**, **76**, 353, 1971.
- Burlaga, L.F., F.B. MacDonald et al., Interplanetary flow systems associated with cosmic ray modulation in 1977 – 1980, **J. Geophys. Res.**, **89**, 6577, 1984.
- Burlaga, L.F., N.F. Ness, Y.-M. Wang, and N.R. Sheeley, Jr., Heliospheric magnetic field strength out to 66 AU: Voyager 1, 1978 – 1996, **J. Geophys. Res.**, **103**, 23,727, 1998.
- Feldman, W.C., Kinetic processes in the solar wind, in *Solar System Plasma Physics, Vol. 1*, Eds. E.N. Parker, C.F. Kennel, and L.J. Lanzerotti, 321, 1979.
- Glassmeier, K.-H., and F.M. Neubauer, Low-frequency electromagnetic plasma waves at Comet P/Grigg-Skjellerup: Overview and spectral characteristics, **J.**

Geophys. Res., **98**, 20,921, 1993.

- Goldstein, M.L., D.A. Roberts, and W.H. Matthaeus, Magnetohydrodynamic turbulence in the solar wind, **Ann. Rev. Astron. Astrophys.**, **33**, 283, 1995.

- Gosling, J.T., J.R. Asbridge et al., Interplanetary ions during an energetic storm particle event: The distribution function from solar wind thermal energies to 1.6 MeV, **J. Geophys. Res.**, **86**, 547, 1981.

- Kennel, C.F., Coroniti, F. V., Scarf, F. L., Livesey, W. A., Russell, C. T., Smith, E. J., A test of Lee's quasi-linear theory of ion acceleration by interplanetary traveling shocks**J. Geophys. Res.**, 91, 11917, 1986.

- Leamon, R.J., C.W. Smith, N.F. Ness, W.H. Matthaeus, and H.K. Wong, Observational constraints on the dynamics of the interplanetary magnetic field dissipation range, **J. Geophys. Res.**, **103**, 4775, 1998.

- Matthaeus, W.H., G.P. Zank, C.W. Smith, and S. Oughton, Turbulence, spatial transport and heating of the solar wind, **Phys. Rev. Lett.**, 82, 3444, 1999.

- Richardson, J.D., K.I. Paularena, A.J. Lazarus, and J.W. Belcher, Evidence for a solar wind slowdown in the outer heliosphere, **Geophys. Res. Lett.**, **22**, 1469, 1995.

- Scholer, M., Diffusive acceleration, in *Collisionless Shocks in the Heliosphere: Reviews of Current Research*, Eds. B.T. Tsurutani and R. G. Stone, AGU, 287, 1985.

- Scholer, M., G. Morfill, and M.A.I. Van Hollebeke, On the origin of corotating energetic particle events, **J. Geophys. Res.**, **85**, 1743, 1980.

- Scholer, M., F.M. Ipavich, G. Gloeckler, and D. Hovestadt, Acceleration of low energy protons and alpha particles at interplanetary shock waves, **J. Geophys. Res.**, **88**, 1977, 1983.

- Smith, E.J., Interplanetary shock phenomena beyond 1 AU, in *Collisionless Shocks in the Heliosphere: Reviews of Current Research*, Eds. B.T. Tsurutani and R. G. Stone, AGU, 69, 1985.